

Relativistic Einstein Rings of Reissner-Nordström Black Holes Nonminimally Coupled to Electrodynamics

Rodrigo Maier*

*Departamento de Física Teórica, Instituto de Física,
Universidade do Estado do Rio de Janeiro,
Rua São Francisco Xavier 524, Maracanã,
CEP20550-900, Rio de Janeiro, Brazil*

(Dated: October 22, 2024)

In this paper we examine the relativistic Einstein rings assuming a nonminimal coupling between gravitation and electromagnetism in a Reissner-Nordström background. Starting from a general action of a nonminimal coupled electrodynamics we show that an unstable effective photon sphere may be obtained in the regime of eikonal approximation. Apart from it, an inner stable photon sphere may also be obtained in the case of large coupling parameters and/or nearly extremal configurations. Restricting ourselves to the outer unstable photon sphere domain we examine the expected angular positions of the first and second relativistic Einstein rings. To compare our results with previous studies in the literature we model the lens as a Galactic supermassive black hole. For fixed coupling parameters we show that such angular positions decrease as the charge parameter increases. The angular separation between the first and second rings is also evaluated. We show that such separation increases as the charge parameter increases. These patterns are not followed by nearly extremal configurations. In this case we show that there is an overlap domain so that the angular position and the corresponding coupling parameter do not allow one to differ extremal cases from complementary configurations which satisfy the cosmic censorship hypothesis.

I. INTRODUCTION

Since the advent of black hole classical solutions[1–5] the behaviour of photon dynamics in a high energy regime has been exhaustively studied. In this context, the deflection of light rays – due to strong gravitational field – with impact factor of the order of the black hole photon sphere may furnish attractive configurations in which high energy physics can be put to the test. In this case, the position of the source with respect to the optical axis plays a significant role by defining the lensing configuration. In the minimal coupling case several studies addressed the lensing at large deflection angles[6–11]. In this scenario, photons may reach a region sufficiently close to the unstable photon sphere so that they may go around the lens a number of times. For the case in which the source, lens and observer are aligned, an infinite number of relativistic Einstein rings may be formed due to the bending of light rays larger than 2π . In the misaligned case on the other hand, an infinite sequence of relativistic images is produced on both sides of the optical axis.

Extending the above mentioned systems, the lensing at large deflection angles has also been examined[12] in the context of a nonminimal coupling between gravitation and the electrodynamic field. From a theoretical ground there are several reasons behind the assumption of such nonminimal coupling. Among them we can mention the obtention of asymptotically flat black hole solutions with a positive ADM mass[13], the effect of vacuum polariza-

tion on magnetic fields around a static black hole[14] and exact cosmological solutions which describe isotropization processes[15]. For a complete review on general couplings between the electromagnetic field and gravitation see [16] and references therein. In this paper we intend to extend the results obtained in [12] considering the case in which the lens is described by a Galactic supermassive black hole with a nonvanishing charge parameter.

Although it is believed that charged black holes are rather unlikely to be observed in nature once they tend to attract opposite charges from their neighbourhood to neutralize themselves, a number of works have been developed in order to better understand proper mechanisms of charged black hole neutralization (see e.g. [17–20] and references therein). From an astrophysical point of view it has been argued that binary black holes may admit electric charge. In fact, according to Zhang’s mechanism[21] a rotating charged black hole may develop a magnetosphere which should allow a nonvanishing charge parameter for a large period of time. The overall effect of such mechanism could provide a signature of an electromagnetic signal in gravitational wave events of binary black hole merger. Further analyses have given support to electric charges in black holes considering electromagnetic counterparts of black hole mergers[22–26]. In the context of this paper we aim to examine the simplest configuration in which a nonrotating black hole with nonvanishing charge parameter changes the angular position of relativistic Einstein rings considering a nonminimal coupling between gravitation and the electromagnetic field.

We organize the paper as follows. In the next section we obtain an effective metric from a Reissner-Nordström background nonminimal coupled to electrodynamics in

*rodrigo.maier@uerj.br

the regime of eikonal approximation. In Section III effective photon spheres are obtained. In Section IV we obtain the angular position of the first and second Einstein relativistic rings modeling our lens by a Galactic supermassive black hole with a charge parameter. In Section V we leave our final remarks.

II. EFFECTIVE GEOMETRY FROM NONMINIMAL COUPLING

We start by considering an action of a general nonminimal coupled electrodynamics

$$\begin{aligned} S_\gamma = & \int \sqrt{-g} F_{\mu\nu} F^{\mu\nu} d^4x \\ & + \int \sqrt{-g} (\gamma_1 R F_{\mu\nu} F^{\mu\nu} + \gamma_2 R_{\mu\nu} F^\mu{}_\beta F^{\nu\beta} \\ & \quad + \gamma_3 R_{\mu\nu\beta\sigma} F^{\mu\nu} F^{\beta\sigma}) d^4x, \end{aligned} \quad (1)$$

where $R_{\mu\nu\beta\sigma}$ is the Riemann tensor $-R_{\mu\nu}$ and R are the Ricci tensor and the Ricci scalar, respectively $-\gamma_i$ ($i = 1, 2, 3$) are coupling coefficients and $F_{\mu\nu} = A_{\nu,\mu} - A_{\mu,\nu}$ is the Faraday tensor with A_μ as the potential 4-vector.

Variations of S_γ with respect A_μ yields the following equations of motion

$$\begin{aligned} \nabla_\mu F^{\mu\nu} + \nabla_\mu \left[\gamma_1 R F^{\mu\nu} + \frac{\gamma_2}{2} (R^\mu{}_\beta F^{\beta\nu} - R^\nu{}_\beta F^{\beta\mu}) \right. \\ \left. + \gamma_3 R^{\mu\nu}{}_{\beta\sigma} F^{\beta\sigma} \right] = 0, \end{aligned} \quad (2)$$

where ∇_α denotes the covariant derivative. Finally, from Bianchi identities we obtain the auxiliary conditions

$$\nabla_\alpha F_{\mu\nu} + \nabla_\mu F_{\nu\alpha} + \nabla_\nu F_{\alpha\mu} = 0. \quad (3)$$

In the following we aim to examine the photon dynamics which emerge from (2)–(3) in a high energy domain engendered from a black hole background. In this context, the propagation of small perturbations of the electromagnetic field around such background can be studied by means of the eikonal approximation in which the test electromagnetic field is given by

$$F_{\mu\nu} = f_{\mu\nu} e^{i\theta}. \quad (4)$$

In the above, θ stands for a very rapidly varying phase compared to the amplitude $f_{\mu\nu}$ when one takes into account scales much higher than the Compton wavelength of the electron. Defining $k_\mu = \theta_{,\mu}$, equation (2) furnishes

$$\begin{aligned} k_\mu (1 + \gamma_1 R) f^{\mu\nu} + \frac{\gamma_2}{2} k_\mu (R^\mu{}_\beta f^{\beta\nu} - R^\nu{}_\beta f^{\beta\mu}) \\ + \gamma_3 k_\mu R^{\mu\nu}{}_{\beta\sigma} f^{\beta\sigma} = 0. \end{aligned} \quad (5)$$

On the other hand, from (3) we obtain

$$k_\alpha f_{\mu\nu} + k_\mu f_{\nu\alpha} + k_\nu f_{\alpha\mu} = 0, \quad (6)$$

so that

$$k^2 f_{\mu\nu} + k_\alpha (k_\nu f_\mu^\alpha - k_\mu f_\nu^\alpha) = 0, \quad (7)$$

where $k^2 \equiv k^\alpha k_\alpha$.

Substituting (5) in the above, we end up with

$$\begin{aligned} k^2 f_{\mu\nu} + \frac{k_\alpha}{1 + \gamma_1 R} \left\{ \frac{\gamma_2}{2} [(k_\nu R_{\mu\beta} - k_\mu R_{\nu\beta}) f^{\beta\alpha} \right. \\ \left. + R^\alpha{}_\beta (k_\mu f_\nu^\beta - k_\nu f_\mu^\beta)] \right. \\ \left. + \gamma_3 (k_\mu R^\alpha{}_{\nu\beta\sigma} - k_\nu R^\alpha{}_{\mu\beta\sigma}) f^{\beta\sigma} \right\} = 0. \end{aligned} \quad (8)$$

Using standard coordinates $x^\alpha = (t, r, \theta, \phi)$ the Reissner-Nordström line element can be written in the base of 1-forms as

$$ds^2 = \eta_{AB} \Theta^A \Theta^B, \quad (9)$$

where

$$\Theta^A = e^A{}_\alpha dx^\alpha, \quad (10)$$

and

$$e^A{}_\alpha \rightarrow \text{diag} \left(f(r), \frac{1}{f(r)}, r, r \sin \theta \right), \quad (11)$$

with

$$f(r) \equiv \sqrt{1 - \frac{2M}{r} + \frac{Q^2}{r^2}}. \quad (12)$$

It is then easy to show that the Riemann tensor reads

$$\begin{aligned} R^\alpha{}_{\beta\gamma\delta} = & h_1(r) \{ \delta^\alpha_\gamma g_{\beta\delta} - \delta^\alpha_\delta g_{\beta\gamma} \\ & + 3[h_2(r) V^\alpha_\beta V_{\gamma\delta} - h_3(r) W^\alpha_\beta W_{\gamma\delta}] \}, \end{aligned} \quad (13)$$

where

$$V^{AB} = \sqrt{-g^{tt} g^{rr}} (e^A{}_t e^B{}_r - e^A{}_r e^B{}_t), \quad (14)$$

$$W^{AB} = \sqrt{g^{\theta\theta} g^{\phi\phi}} (e^A_\theta e^B_\phi - e^A_\phi e^B_\theta), \quad (15)$$

and

$$h_1(r) = \frac{M}{r^3} - \frac{Q^2}{r^4}, \quad (16)$$

$$h_2(r) = 1 + \frac{Q^2}{3(Q^2 - Mr)}, \quad (17)$$

$$h_3(r) = 1 - \frac{Q^2}{3(Q^2 - Mr)}. \quad (18)$$

The substitution of (13) in (8) – and further contraction with $V^{\mu\nu}$ – furnishes a modified light cone[12, 27] dictated by

$$(1 - \Sigma)(k_t k^t + k_r k^r) + k_\theta k^\theta + k_\phi k^\phi = 0. \quad (19)$$

In this case, photons are expected to follow an effective geometry[28] whose line element reads

$$\begin{aligned} d\tilde{s}^2 &= \tilde{g}_{\mu\nu} dx^\mu dx^\nu \\ &= \left(1 - \frac{1}{x} + \frac{q^2}{x^2}\right)(1 - \Sigma) dT^2 \\ &\quad - \left(1 - \frac{1}{x} + \frac{q^2}{x^2}\right)^{-1} (1 - \Sigma) dx^2 \\ &\quad - x^2(d\theta^2 + \sin^2 \theta d\phi^2), \end{aligned} \quad (20)$$

where

$$T = \frac{t}{2M}, \quad x = \frac{r}{2M}, \quad q = \frac{Q}{2M}, \quad (21)$$

$$\Gamma_2 = \frac{\gamma_2}{(2M)^2}, \quad \Gamma_3 = \frac{\gamma_3}{(2M)^2}, \quad (22)$$

and

$$\Sigma \equiv \frac{3x\Gamma_3 - q^2(\Gamma_2 + 8\Gamma_3)}{x^4 + \Gamma_3(x - 2q^2)}. \quad (23)$$

III. EFFECTIVE PHOTON SPHERES

To proceed we now investigate the motion of photons subjected to the effective geometry (20). The equations of motion are

$$\frac{d^2 x^\mu}{d\sigma^2} + \tilde{\Gamma}_{\alpha\beta}^\mu \frac{dx^\alpha}{d\sigma} \frac{dx^\beta}{d\sigma} = 0, \quad (24)$$

where we regard $\tilde{\Gamma}_{\alpha\beta}^\mu$ as the Christoffel connection built with the effective geometry $\tilde{g}_{\mu\nu}$ and σ is a proper affine parameter. To simplify our analysis we restrict ourselves orbits with initial conditions $\theta_0 = \pi/2$ and $d\theta/d\sigma|_0 = 0$. In this case it can be shown that the dynamics is restricted in the equatorial plane and one can obtain two constants of motion,

$$E = \left(1 - \frac{1}{x} + \frac{q^2}{x^2}\right)(1 - \Sigma) \left(\frac{dT}{d\sigma}\right), \quad L = x^2 \left(\frac{d\phi}{d\sigma}\right), \quad (25)$$

connected to the energy and angular momentum, respectively.

Substituting the above results in the first integral

$$\tilde{g}_{\mu\nu} \frac{dx^\mu}{d\sigma} \frac{dx^\nu}{d\sigma} = 0, \quad (26)$$

we obtain

$$(1 - \Sigma)^2 \left(\frac{dx}{d\sigma}\right)^2 + U_{eff}(x) = E^2, \quad (27)$$

where

$$U_{eff}(x) = \frac{L^2 \left(1 - \frac{1}{x} + \frac{q^2}{x^2}\right)(1 - \Sigma)}{x^2}. \quad (28)$$

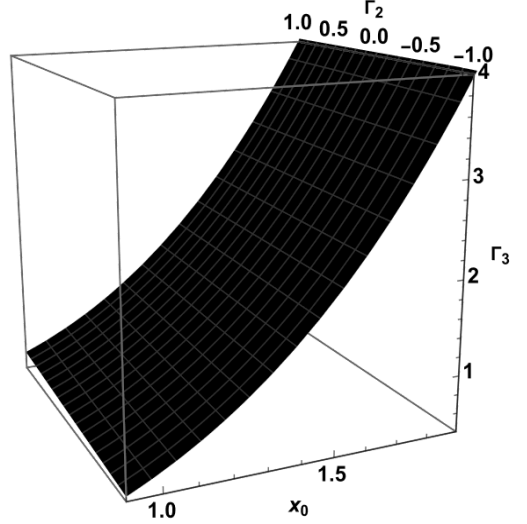


FIG. 1: The behaviour of Γ_3 with respect to x_0 in the domain $-1 \leq \Gamma_2 \leq 1$. For a fixed Γ_2 there is a $x_0 > x_h$ allowing the formation of an inner stable photon sphere as long as $\Gamma_3 \gtrsim 0.6$.

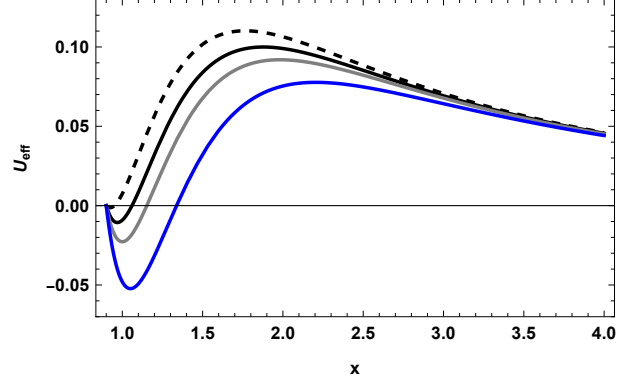


FIG. 2: The behaviour of the effective potential in the domain $x > x_h$ for different values of Γ_3 . $\Gamma_3 = 0.6$ (black dashed), $\Gamma_3 = 0.8$ (black bold), $\Gamma_3 = 1.0$ (grey), $\Gamma_3 = 1.5$ (blue). While the maximum of the effective potential furnishes the usual unstable photon sphere, its minimum defines an inner stable photon sphere. In this plot we have fixed $\Gamma_2 = 0$.

The maximum of the effective potential U_{eff} defines the photon sphere. For $\Sigma = 0$ we obtain

$$x_{RN} = \frac{3 + \sqrt{9 - 32q^2}}{4} \quad (29)$$

denoting the Reissner-Nordström unstable photon sphere as one should expect. Moreover, defining

$$x_h = \frac{1 + \sqrt{1 - 4q^2}}{2} \quad (30)$$

as the Reissner-Nordström event horizon, it can be easily shown from (28) that

$$U_{eff}(x_h) = 0. \quad (31)$$

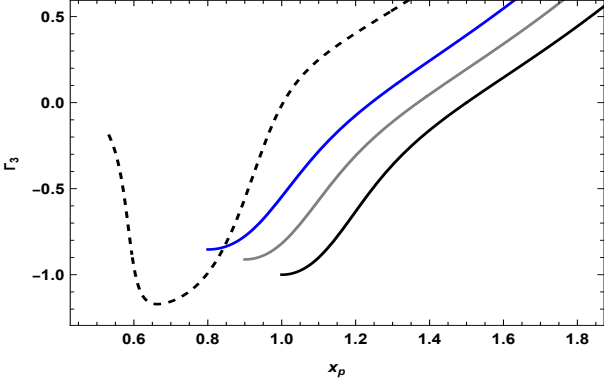


FIG. 3: Γ_3 as a function of x_p for different charge parameters in the domain $x > x_h$. The solid black, gray and blue curves are connected to $q = 0$, $q = 0.3$ and $q = 0.4$, respectively. The black dashed curve on the other hand is connected to a nearly extremal configuration in which $q \simeq 0.5$. In this case one may notice that apart from an outer unstable photon sphere, there is also an inner stable photon sphere in the domain $\Gamma_3 \lesssim -0.2$.

Furthermore, once

$$\lim_{x \rightarrow +\infty} U_{eff}(x) = 0 \quad (32)$$

and $dU_{eff}/dx \simeq -2L^2/x^3 < 0$ for large x one may notice that U_{eff} has at least one unstable photon sphere analogous to that of the Reissner-Nordström spacetime. In fact, for a negligible charge and small coupling parameters Γ_2 and Γ_3 this is the sole formed photon sphere. To see this behaviour, let us consider an expansion of U_{eff} up to first order in the coupling parameters. That is,

$$U_{eff}(x) \simeq \left(\frac{L}{x^3}\right)^2 \left(1 - \frac{1}{x} + \frac{q^2}{x^2}\right) \times [x^4 - 3x\Gamma_3 + q^2(\Gamma_2 + 8\Gamma_3)]. \quad (33)$$

Assuming a sufficiently small charge and coupling parameters, namely q , Γ_2 and $\Gamma_3 \ll 1$, it can be shown that

$$\frac{dU_{eff}}{dx} \simeq -L^2 \left[\frac{2x^6 - 3x^5 + 4q^2x^4 - 3\Gamma_3x^2(5x - 6)}{x^9} \right] \quad (34)$$

In this approximation it is then easy to show that the effective potential has one global maximum connected to the effective unstable photon sphere located at

$$\tilde{x}_p = x_{RN} + \delta \quad (35)$$

where

$$\delta = \frac{3x_{RN}(5x_{RN} - 6)\Gamma_3}{x_{RN}^3(4x_{RN} - 3) + 18(5x_{RN} - 7)\Gamma_3}. \quad (36)$$

A more interesting behaviour may be notice assuming the case of large coupling parameters. To this end, let us consider the full effective potential (28) with no approximations. Assuming that

$$x_0^4 - 2\Gamma_3x_0 + q^2(\Gamma_2 + 6\Gamma_3) = 0 \quad (37)$$

for some $x_0 > x_h$, the effective potential will display a global minimum so that an inner stable photon sphere may be formed. To illustrate this behaviour, let us write the solution of (37) as

$$\Gamma_3 = \frac{-x_0^4 - q^2\Gamma_2}{2(3q^2 - x_0)}. \quad (38)$$

Considering the domain $0 \leq q \leq 0.5$, we fix a typical value for the charge, namely, $q = 0.3$. In Fig. 1 we show the behaviour of Γ_3 with respect to x_0 in the domain $-1 \leq \Gamma_2 \leq 1$. Here we see that for a fixed Γ_2 , there is a $x_0 > x_h$ as long as $\Gamma_3 \gtrsim 0.6$. In Fig. 2 we show the behaviour of the effective potential in the domain $x > x_h$ for different values of Γ_3 fixing $\Gamma_2 = 0.0$. For $\Gamma_3 \gtrsim 0.6$ we see that the effective potential develops a global minimum connected to an inner stable photon sphere.

A similar behaviour may be notice considering the case of nearly extremal configurations and smaller coupling parameters. In fact, fixing $\Gamma_2 = 0$ for instance, the equation

$$\frac{dU_{eff}}{dx} \Big|_{x_p} = 0 \quad (39)$$

furnishes the coupling parameter Γ_3 as a function of the photon sphere position x_p and the charge parameter q . In Fig. 3 we show the behaviour of Γ_3 as a function of x_p according to (39) for different charge parameters. The black, gray and blue curves – configurations far from the extremal case – furnish a sole unstable photon sphere as one should expect since $\Gamma_3 \lesssim 0.6$. On the other hand, the black dashed curve with $q \simeq 0.5$ allows two different solutions for $\Gamma_3 \lesssim -0.2$. It can be easily shown that these solutions are connected to an inner stable photon sphere and an outer unstable photon sphere.

IV. RELATIVISTIC EINSTEIN RINGS

We now examine the strong gravitational lensing connected to the effective geometry (20). To this end we assume that photons reach a region sufficiently close to the outer unstable photon sphere so that they may go around the lens an number of times. Considering that the source, lens and observer are aligned, an infinite number of relativistic Einstein rings are formed due to the bending of light rays larger than 2π . In order to provide a model to sketch the source, lens and observer configuration we are going to adhere to the lens equation proposed by K. S. Virbhadra and G. F. R. Ellis[8]. In this context we shall assume that both observer and source are located in asymptotically flat regions sufficiently far from the lens. The line connecting the observer, the lens and the source defines the optical axis. Denoting θ as the angle of the source's image with respect to the optic axis and α as the Einstein deflection angle, the lens equations reads

$$\tan \theta = \frac{D_{LS}}{D_S} [\tan \theta + \tan(\alpha - \theta)], \quad (40)$$

where D_{LS} is the lens-source distance and D_S is the distance of the source from the observer. In this context the impact factor J can be written as[8, 12]

$$J = D_L \sin \theta. \quad (41)$$

On the other hand, according to standard calculations the Einstein deflection angle in our case is given by

$$\alpha = 2 \int_{x_c}^{\infty} \frac{\sqrt{1 - \Sigma(x)} dx}{x \sqrt{\frac{x^2}{x_c^2} \left(1 - \frac{1}{x_c} + \frac{q^2}{x_c^2}\right) \frac{1 - \Sigma(x_c)}{1 - \Sigma(x)} - \left(1 - \frac{1}{x} + \frac{q^2}{x^2}\right)}} - \pi, \quad (42)$$

while the impact factor reads

$$J = \frac{2Mx_c}{\sqrt{\left(1 - \frac{1}{x_c} + \frac{q^2}{x_c^2}\right)(1 - \Sigma(x_c))}}. \quad (43)$$

In the above x_c is the closest distance of approach.

To compare our results with those obtained in the literature[8, 12] we shall model the lens as a Galactic supermassive black hole with a nonvanishing charge. To this end we shall fix the parameters

$$D_L = 8.5 \text{ Kpc}, \quad M = 2.8 \times 10^6 M_\odot, \quad D_S = 2D_{LS} \quad (44)$$

where M_\odot is the Solar mass. Moreover, in order to simplify our analysis from now on we shall fix $\Gamma_2 = 0$. In fact, according to (23) one may notice that the coupling parameter Γ_2 plays a role of an additive constant – together with Γ_3 – connected to the black hole charge. Bearing this feature in mind we expect that the following results should hold, from a qualitative point of view, for a nonvanishing Γ_2 and in a similar domain of Γ_3 .

Following the standard route shown in [8, 12] we are then in a position to evaluate the angular position of the first and second relativistic Einstein rings. In Fig. 4 we show the angular positions of the first (top panel) and second (bottom panel) relativistic Einstein rings considering several charge parameters as a function of Γ_3 . Here we see that the angular positions decrease as the charge parameter increases.

Defining

$$\theta_1 = \theta - 2\pi \quad \text{and} \quad \theta_2 = \theta - 4\pi \quad (45)$$

as the angular position of the first and second relativistic Einstein ring respectively, we introduce the separation parameter as

$$\delta\theta = \theta_1 - \theta_2. \quad (46)$$

In Fig. 5 we show that the separation parameter increases as the charge parameter increases.

Based on the numerical simulations of Figs. 4 and 5 we see that the above mentioned patterns cannot be extended up to nearly extremal configurations. In fact,

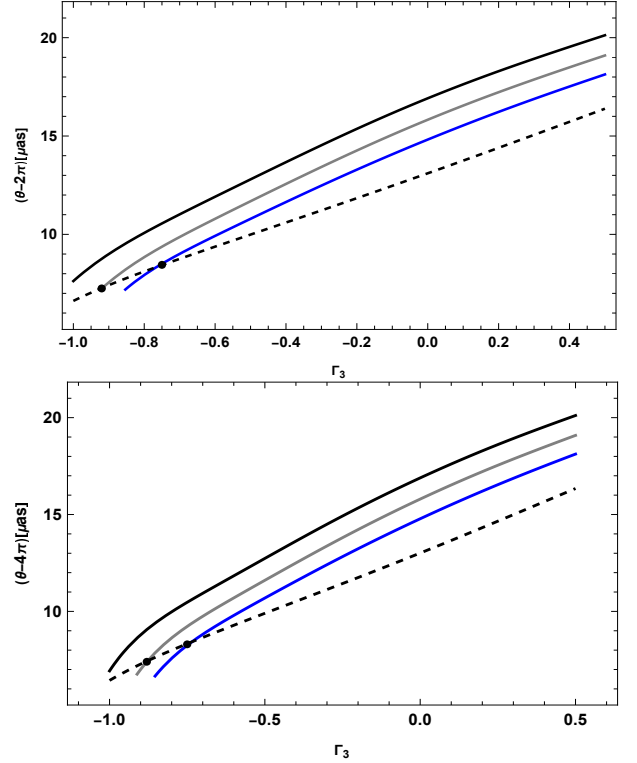


FIG. 4: The angular positions of the first (top panel) and second (bottom panel) relativistic Einstein rings as a function of Γ_3 for several charge parameters. The solid black, gray and blue curves are connected to $q = 0.0$, $q = 0.3$ and $q = 0.4$, respectively. Here we see that the angular position decreases as the charge parameter increases. The black dashed curve is connected to the nearly extremal configuration in which $q \simeq 0.5$. The black solid dots are examples of points of the domain of overlap of nearly extremal configurations and the complementary ones.

according to our numerical examples one may notice that there is a domain of overlap between nearly extremal configurations and the complementary ones which respect the cosmic censorship hypothesis. Examples of such overlaps are illustrated in Figs. 4 and 5 by the solid black dots. In this case the angular position together with its corre-

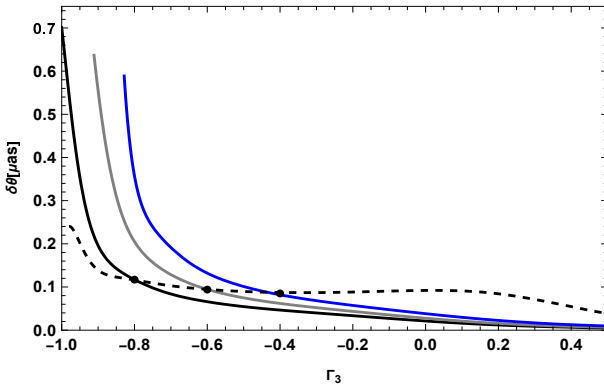


FIG. 5: The separation parameter $\delta\theta$ as a function of Γ_3 for several charge parameters. The solid black, gray and blue curves are connected to $q = 0.0$, $q = 0.3$ and $q = 0.4$, respectively. Here we see that the separation parameter increases as the black hole charge increases. The black dashed curve is connected to the nearly extremal configuration in which $q \simeq 0.5$. Again, the black solid dots are examples of points of the domain of overlap of nearly extremal configurations and the complementary ones.

ponding coupling parameter do not allow one to differ nearly extremal cases from configurations far from those.

V. FINAL REMARKS

In this paper we have examined strong lensing configurations assuming a nonminimal coupling between gravitation and electromagnetism in a Reissner-Norström background. From an eikonal approximation we show that photons follow an effective geometry which allows the formation of an effective unstable photon sphere. Apart from it, for a large domain of the coupling parameters/nearly extremal configurations a inner stable photon sphere may also be obtained. In order to simplify our analysis we restrict ourselves to the case in which photons reach a sufficiently close distance from the outer

unstable photon sphere so that relativistic Einstein rings can be observed once the source, lens and the observer are aligned. To compare our results to those in the literature we model the lens as a Galactic supermassive black hole with a nonvanishing electric charge. For fixed coupling parameters we show that the angular positions of the first and second Einstein relativistic rings decrease as the charge parameter increases. On the contrary, for fixed coupling parameters the separations between the first and second Einstein rings increase as the charge parameter increases. We show that these patterns cannot be extended up to nearly extremal configurations. In this case we show that there is an overlap domain in which the angular position together with its corresponding coupling parameter do not fix the black hole charge.

From an observational point of view it is worth to remark that the highest resolution telescope available today[29] has a resolution of the order of $19\mu\text{as}$. Taking into account our results shown in Sec. IV we notice that the actual angular positions of the first and second relativistic Einstein rings in Fig. 4 may put a better constrain on the coupling parameter Γ_3 rather than their separations in Fig. 5. An additional difficulty to fix such constrain should be a proper method to infer the overall black hole charge. Nevertheless, the inceptive results presented here show that it may be feasible in the future to put better limits on the coupling parameters. Of course the theoretical estimates presented in this paper may improve if different/more general configurations are considered. In this context, different ratios D_{LS}/D_S and/or misaligned configurations could provide a better screening for the allowed values for the coupling parameters.

Finally, the analysis presented in our paper should be extended to more general cases such as Kerr black holes. Configurations in which the lens is modeled by a boosted black hole[30] could also furnish a more realistic system to be faced to observations. We shall examine these subjects in our further research.

[1] K. Schwarzschild, *Sitzungsber. Preuss. Akad. Wiss. Berlin (Math. Phys.)* **1916**, 189-196 (1916). [arXiv:physics/9905030 [physics]].

[2] H. Reissner, *Annalen Phys.* **355**, no.9, 106-120 (1916).

[3] G. Nordström, *Koninklijke Nederlandse Akademie van Wetenschappen Proceedings*, vol. 20, iss. 2, p.1238-1245 (1918).

[4] R. P. Kerr, *Phys. Rev. Lett.* **11**, 237-238 (1963).

[5] E. T. Newman, R. Couch, K. Chinnapared, A. Exton, A. Prakash and R. Torrence, *J. Math. Phys.* **6**, 918-919 (1965).

[6] V. Perlick, *Living Rev. Rel.* **7**, 9 (2004).

[7] V. Bozza, *Gen. Rel. Grav.* **42**, 2269-2300 (2010) [arXiv:0911.2187 [gr-qc]].

[8] K. S. Virbhadra and G. F. R. Ellis, *Phys. Rev. D* **62**, 084003 (2000) [arXiv:astro-ph/9904193 [astro-ph]].

[9] K. S. Virbhadra, *Phys. Rev. D* **79**, 083004 (2009) [arXiv:0810.2109 [gr-qc]].

[10] E. F. Eiroa, G. E. Romero and D. F. Torres, *Phys. Rev. D* **66**, 024010 (2002) [arXiv:gr-qc/0203049 [gr-qc]].

[11] T. Hsieh, D. S. Lee and C. Y. Lin, *Phys. Rev. D* **103**, no.10, 104063 (2021) [arXiv:2101.09008 [gr-qc]].

[12] S. E. P. Bergliaffa, E. E. d. Filho and R. Maier, *Phys. Rev. D* **101**, no.12, 124038 (2020) [arXiv:2006.02162 [gr-qc]].

[13] F. Mueller-Hoissen and R. Sippel, *Class. Quant. Grav.* **5**, 1473 (1988)

[14] P. Pavlović and M. Sossich, *Phys. Rev. D* **99**, no.2, 024011 (2019) [arXiv:1809.06054 [gr-qc]].

[15] A. B. Balakin and W. Zimdahl, *Phys. Rev. D* **71**, 124014

(2005) [arXiv:astro-ph/0504228 [astro-ph]].

[16] A. B. Balakin and J. P. S. Lemos, *Class. Quant. Grav.* **22**, 1867-1880 (2005) [arXiv:gr-qc/0503076 [gr-qc]].

[17] D. M. Eardley and W. H. Press, *Ann. Rev. Astron. Astrophys.* **13**, 381-422 (1975).

[18] R. Ruffini, G. Vereshchagin and S. S. Xue, *Phys. Rept.* **487**, 1-140 (2010) [arXiv:0910.0974 [astro-ph.HE]].

[19] D. i. Hwang and D. h. Yeom, *Phys. Rev. D* **84**, 064020 (2011) [arXiv:1010.2585 [gr-qc]].

[20] Y. Gong, Z. Cao, H. Gao and B. Zhang, *Mon. Not. Roy. Astron. Soc.* **488**, no.2, 2722-2731 (2019) [arXiv:1907.05239 [gr-qc]].

[21] B. Zhang, *Astrophys. J. Lett.* **827**, no.2, L31 (2016) [arXiv:1602.04542 [astro-ph.HE]].

[22] S. L. Liebling and C. Palenzuela, *Phys. Rev. D* **94**, no.6, 064046 (2016) [arXiv:1607.02140 [gr-qc]].

[23] T. Liu, G. E. Romero, M. L. Liu and A. Li, *Astrophys. J.* **826**, no.1, 82 (2016) [arXiv:1602.06907 [astro-ph.HE]].

[24] B. Punsly and D. Bini, *Mon. Not. Roy. Astron. Soc.* **459**, no.1, L41-L45 (2016) [arXiv:1603.05509 [astro-ph.HE]].

[25] J. Levin, D. J. D’Orazio and S. Garcia-Saenz, *Phys. Rev. D* **98**, no.12, 123002 (2018) doi:10.1103/PhysRevD.98.123002 [arXiv:1808.07887 [astro-ph.HE]].

[26] C. M. Deng, Y. Cai, X. F. Wu and E. W. Liang, *Phys. Rev. D* **98**, no.12, 123016 (2018) [arXiv:1812.00113 [astro-ph.HE]].

[27] I. T. Drummond and S. J. Hathrell, *Phys. Rev. D* **22**, 343 (1980).

[28] C. Barcelo, S. Liberati and M. Visser, *Living Rev. Rel.* **8**, 12 (2005) [arXiv:gr-qc/0505065 [gr-qc]].

[29] Alexander W. Raymond *et al* 2024 *AJ* **168** 130.

[30] R. F. Aranha, C. E. Cedeño M., R. Maier and D. Soares, *Phys. Rev. D* **103**, no.6, 064060 (2021) [arXiv:2102.01660 [gr-qc]].